Iranian Journal of Physics Research, Vol. 25, No. 3, 2025
DOI: 10.47176/ijpr.25.3.12007

# Effective removal of chromium (VI) via modified maghemite nanoparticles: role of surfactant structure

**Belabed Kherfia[1,2], Naous Mohamed[1,2*], Djeffal Imane[1], Halfadji Ahmed[1,3], Bounaceur Boumediene[2]**
[1]Department of Sciences and Technology, Faculty of Applied Sciences
Ibn Khaldoun University, Tiaret, 14000, Algeria
[2]Macromolecular Physicochemical Laboratory, University of Oran1 Ahmed Ben Bella, Oran, Algeria
[3]Synthesis and Catalysis Laboratory, Ibn Khaldoun University of Tiaret,Tiaret, 14000, Algeria.

E-mail: mohamed.naous@univ-tiaret.dz

(Received 13 November 2024 ; in final form 04 October 2025)

**Abstract**
This study investigates the use of maghemite nanoparticles (MNPs) for the effective removal of hexavalent chromium (Cr(VI)) from wastewater. To improve the adhesion properties of MNPs, alkyl trimethyl ammonium bromide (CnTAB) surfactants were incorporated into the nanoparticles. The modified nanoparticles, referred to as MNPs@CnTAB or γ-$Fe_2O_3$@CnTAB, were characterized using FTIR, TEM, and XRD techniques. To assess theimpact of various parameters on chromium removal, batch experiments were statistically designed, focusing on solution pH, initial Cr(VI) concentration, added salt, adsorbent dosage, and CnTAB chain length. Results showed that both longer surfactant chains and higher adsorbent dosages enhanced removal efficiency. Under optimized conditions—including specific pH, adsorbent dosage, and an initial Cr(VI) concentration of 1 mg/L—a removal efficiency of up to 96% was achieved. These findings demonstrate that MNPs@CnTAB nanomaterials are a promising, environmentally friendly option for the treatment of chromium-contaminated water. This approach supports the development of advanced materials for sustainable water purification and highlights the influence of surfactant structure on nanoparticle performance.

**Keywords:** Chromium removal; maghemite nanoparticles; CnTAB; FTIR; XRD

## 1. Introduction

The poisonous and carcinogenic qualities of chromium present a serious threat to the environment and human health when present in water sources [1]. In order to guarantee the security of drinking water sources, effective and affordable techniques for eliminating chromium ions from water are essential [2]. Since it can remove contaminants more effectively and efficiently, nanotechnology has become a viable water treatment method. Functionalized nanoparticles have drawn a lot of interest in the purification of water.

Maghemite (γ-$Fe_2O_3$) nanoparticles are one kind of nanoparticle that has demonstrated significant promise in water treatment [3]. Because of their special qualities, which include their large surface area, chemical stability, and magnetic activity, maghemite nanoparticles are a great option for a number of uses, including the removal of pollutants [4]. However, surface functionalization is frequently required to increase their affinity and selectivity towards particular pollutants [5]. The functionalization of nanoparticles has made extensive use of cationic surfactants due to their many benefits, which include stability, ease of production, and adjustable surface characteristics. Alkyl trimethyl ammonium bromide (CnTAB) is one of these surfactants whose potential for use in water treatment applications has been well studied[6-9]. Improved chromium removal results from the manipulation of nanoparticle characteristics such a surface charge, hydrophobicity, and dispersibility with the use of CnTAB with different chain lengths[10].

Recent advancements related to the efficiency, adsorption mechanisms, and practical applications of such nanoparticles in wastewater treatment [11-14]. Notably, studies by Li et al. (2022), Zhao et al. (2023).

This work focuses on the preparation and characterization of maghemite nanoparticles functionalized with three distinct cationic surfactants that have varied CnTAB chain lengths. A coprecipitation approach is used to manufacture the nanoparticles, guaranteeing a homogeneous distribution of surfactants on the nanoparticle surface [15].

The theory behind the choice of surfactant chain length is that it will alter the hydrophobicity and surface charge of

the nanoparticles, which will in turn affect their ability to adsorb chromium [16, 17].

The specific goals of the study are as follows: (i) to synthesize MNPs through a straightforward and cost-efficient approach, and to characterize their structural and chemical properties using X-ray diffraction (XRD) and Fourier-transform infrared spectroscopy (FTIR); (ii) to identify the optimal CnTAB chain length that maximizes the adsorption capacity of MNP-CnTAB composites for chromium removal; and (iii) to investigate the influence of pH and coexisting ions on the adsorption behavior of chromium by the modified nanoparticles [18]. We will assess their stability and absorption capabilities in different experimental setups

The objective of this study is to analyze the effectiveness of functionalized maghemite nanoparticles in the removal of chromium ions from water.

## 2. Experimental section

### 2.1. Materials

The following chemicals were supplied by Merck: trimethyl ammonium bromide (DeTAB), tetradecyl trimethyl ammonium bromide (TTAB), and Hexadecyl trimethyl ammonium bromide(CTAB). Additionally, ammonia ($NH_3$), hydrochloric acid (HCl), perchloric acid ($HClO_4$), ferrous chloride tetrahydrate ($FeCl_2 \cdot 4H_2O$), and ferric chloride hexahydrate ($FeCl_3 \cdot 6H_2O$) were obtained from Merck in France and transported to Kenilworth, NJ, USA.The suppliers of acetone (≥99%), 1,5-diphenylcarbazide (DPC, ≥99%), and hydrochloric acid (HCl, 37%) from Sigma Aldrich. The MNPs were synthesised and rinsed using deionized and double-distilled water.

### 2.2. Synthesis of Alkyl trimethyl ammonium Bromide Coated Maghemite Nanoparticles (MNPs@CnTAB).

Five grams of iron (III) chloride ($FeCl_3$, $6H_2O$), four grams of iron (II) chloride ($FeCl_2$, $4H_2O$), and half a gram of CnTAB were dissolved in sixty milliliters of distilled water while being stirred at 80°C until the mixture completely dissolved. This was the single step used to manufacture CnTAB-functionalized maghemite. The next step involved adding 40 ml of a 15% ammonium hydroxide solution dropwise over 20 minutes, until a dark brown color formed. Stirring continuously, keep the temperature at 80°C for 40 more minutes.

Rinse MNPs@CTAB three times with water. The samples were dried at 50°C in a vacuum oven after being separated using a magnet. Before using them again, keep the MNPs in a glass container [19].

### 2.3. Characterisation

X-ray diffraction (XRD) was performed with a resolution of approximately 0.02° 2θ, an angular range from 10° to 90° 2θ, and a step size of 0.02°, ensuring accurate identification of the crystal structure.The Scherrer formula was used to get the average crystal size [20]

$$d = K\lambda/\beta \cos \theta \quad (1)$$

in which the letter "d" denotes the crystal size, while "K" denotes the Scherrer factor, typically valued at 0.9. The X-ray wavelength of the Cu Kα radiation, 1.5418 Å, is represented by the symbol "λ".

The peak width β in radians (commonly measured as the full width at half maximum, FWHM) is inversely related to the crystallite (Lhkl), which is perpendicular to the h k l plane. The diffraction angle is represented by "θ" [21].

The Fourier transform infrared (FTIR) spectra were recorded using a JASCO FT/IR-4100 spectrometer. The range was 4000.6 - 399.1 cm-1. The morphology of γ-$Fe_2O_3$ was analyzed with a transmission electron microscope using a JEOL JEM1010 instrument operating at 100 kV. pH measurements were taken with a pH-mètre HI 9124 ,Ultrapure Milli-Q (Merck Millipore, Madrid, Spain)water was utilized in all experiments.

### 2.4. Method

A run of the chromium (VI) standard solution containing 100 mg/L was used to create a series of standard solutions containing 0.40, 0.50, 0.60, 0.70, and 0.80 mg/L for the adsorption experiments.

30 ml of distilled water were subjected to different quantities of unfunctionalized γ-$Fe_2O_3$ (4 mg/ml) and γ-$Fe_2O_3$@CnTAB nanoparticles (4, 8, and 12 mg/ml) at pH 2, pH 7, and pH 9. The mixture was immersed in an ultrasonic bath for an hour. Submerged in an ultrasonic bath once more, the mixture was added 0.5 ml of $K_2CrO_4$ solution. At intervals of five, ten, and fifteen minutes, 5 ml samples were taken. For an entire day, these mixes were stored at 4 °C. The samples that were taken the previous day were mixed with 80 ml of distilled water, 20 mL of DPC 1.5 solution and 4 mL of 2 N sulfuric acid. The presence of chromium hexavalent ions in the filtrates was next assessed using UV-Vis spectroscopy (Perkin Elmer lambda 35, Waltham, MA, USA) at 540 nm. The removal of Cr(VI) ions from the solution was shown by the decrease in color intensity.

### 2.5. pH effect

Acidic, neutral, and alkaline pH levels were used in the studies to evaluate the adsorption capacity in different conditions. The samples' pH was changed to 2.0, 7.0, and 9.0 by adding 0.01 N HCl or 0.01 N NaOH. The calibration curve shown above was used to calculate the values of the various Cr(VI) concentrations. The following formula was used to determine the percentage of Cr(VI) removal

$$RE(\%) = (C_0 - Ce)/C_0 * 100 \quad (2)$$

Ehere $C_0$ : Cr (VI) initial concentration (mg/l). Ce: Cr (VI) residual concentration in mg/l.

The previously described calibration curve served as the basis for determining the Cr(VI) concentrations. Equation (2) was used to determine the percentage of Cr(VI) removal. $C_0$ represents the initial Cr(VI) concentration in (mg/L), where Ce represents the remaining Cr(VI) concentration in the solution (mg/L) [22].

### 2.6. Effect of initial Cr(VI) concentration

γ-$Fe_2O_3$@CnTAB nanoparticles were introduced into flasks containing 25 mL of Cr(VI) solution at 8 mg/mL. The adsorption capacity of metal ions onto the γ-$Fe_2O_3$@CnTAB nanoparticles was then calculated using equation (1) and equation (2).

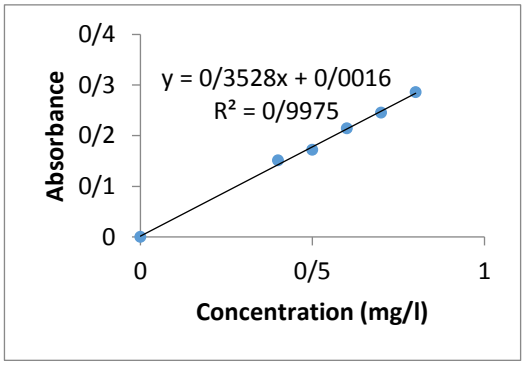


**Figure 1**. Calibration Curve for the Determination of Chromium(VI) Using 1,5-Diphenylcarbazide


**Figure 2.** Formation of maghemite nanoparticles

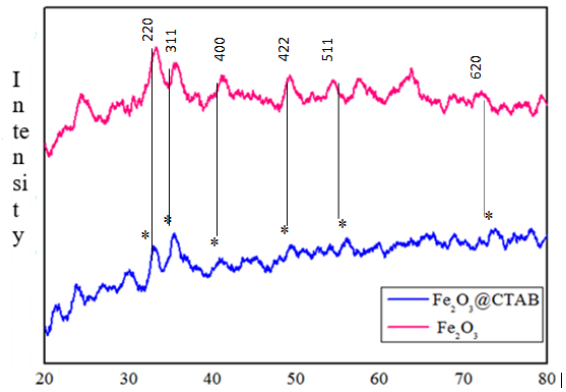


**Figure 3.** XRD patterns of γ-$Fe_2O_3$@CnTAB composite and γ-$Fe_2O_3$ nanoparticles.

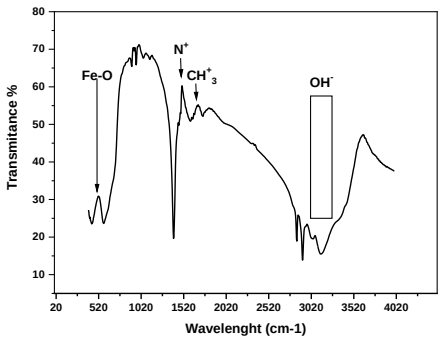


**Figure 4.** FTIR Spectra of γ-Fe2O3@CTAB

### 2.7. Effect of interfering ions

Potassium nitrate salt was used in the experiment to investigate how salt affects Cr(VI) adsorption. 30 milliliters of pH 2 distilled water were mixed with 0.2 grams of γ-$Fe_2O_3$@CnTAB nanoparticles and 0.025 grams of $KNO_3$. For one hour, the mixture was ultrasonically treated. $K_2CrO_4$ solution (0.5 ml) was then added to the mixture. Five milliliter samples were taken at intervals of five, ten, and fifteen minutes, and they were kept at 4°C for a full day. Each of the earlier samples was then mixed with 4 ml of 2 N sulfuric acid, 0.20 ml of DPC solution, and 0.80 ml of ultrapure water. After that, the samples were examined with UV-visible spectroscopy, and each sample's absorbance was calculated [23].

## 3. Results and Discussion

### 3.1. Strucural analysis

#### 3.1.1. XRD

The coprecipitation process produces maghemite with hues ranging from brown to dark brown (figure 2). Figure 3 presents the characteristic XRD pattern of γ-$Fe_2O_3$@CnTAB, with XRD data recorded over a 2-theta range from 10° to 90°. The diffraction patterns in this analysis showed strong alignment with several crystallographic planes, including (220), (311), (400), (422), (511) and (620). These planes closely matched the maghemite phase, indicating that the synthesized γ-$Fe_2O_3$@CnTAB adsorbent contained this specific phase.
The XRD data revealed no evidence of additional phases, confirming the purity of the synthesized product. Furthermore, The diffraction peaks suggest that the material is crystalline [24].

#### 3.1.2. FTIR

The FTIR spectrum of the γ-$Fe_2O_3$@CnTAB nanoparticles indicated an electrostatic interaction between the γ-$Fe_2O_3$ surface ($OH^-$...$N^+$)anda the OH of the ammonium in CnTAB,peaks in the 3300-3060 $cm^{-1}$ range. The peaks at 2840 $cm^{-1}$ and 2915 are attributed to two distinct CH bands of the -$CH_2$ group in CnTAB. The peaks at 1606 and 1408 $cm^{-1}$ correspond to the asymmetric and symmetric stretching oscillationsof $N^+$ $CH_3$, respectively. Additionally, The peak at 956 $cm^{-1}$ is attributed to the out-of-plane $CH_3$ vibration, while a prominent peak at 580 $cm^{-1}$ signifiesthe stretching vibration of the Fe-O bond in γ-$Fe_2O_3$ [25].
Understanding the chemical interactions and vibrational features of γ-$Fe_2O_3$@CnTAB nanoparticles is crucial for comprehending their surface and structural characteristics, since these studies shed light on them.

#### 3.1.3.TEM

The TEM image in Figure 4 displays spherical particles with sizes between 10 and 20 nm. The average crystallite size, determined using the Debye-Scherrer formula, was about 14 nm, which is in agreement with values reported in previous studies [26]. The calculation Debye-Scherrer formula resulted in an average crystallite size of about 14 nm.

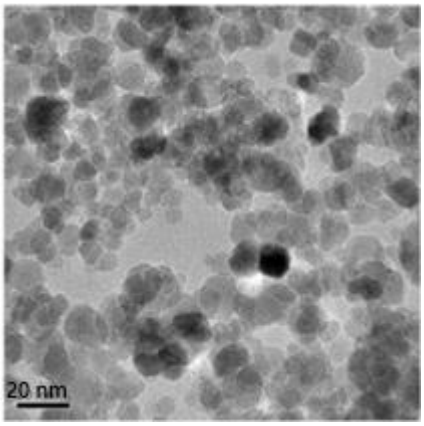


Figure 5. TEM images of maghemite nanoparticles for γ-$Fe_2O_3$@CTAB

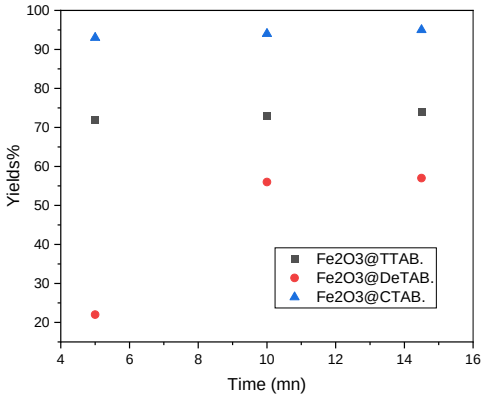


**Figure 6.** % removal of Cr(VI) by different γ-$Fe_2O_3$@CnTAB.

Remarkably, the γ-$Fe_2O_3$ particle sizes determined from the XRD pattern using the Scherrer equationand those shown in the TEM image showed good agreement.

### 3.2. Effect of functionalization on adsorption

The findings show that the proportion of chromium (VI) eliminated is not higher than 73%. This mean outcome might be the consequence of the instability of nonfunctionalized maghemite nanoparticles, which lowers the ratio of surface area to volume and, in turn, lowers the amount of adsorption on these surfaces. On the other hand, γ-$Fe_2O_3$@CTAB, surfactant-functionalized nanoparticles, eliminate Cr(VI) with a 97% removal efficiency. The section that follows gives an example of this.

### 3.3. Effect of chain length

The following yields were obtained in an acidic medium at pH 2, using a constant concentration of γ-$Fe_2O_3$@CnTAB (4 mg/mL) and time intervals of 5, 10, and 15 minutes (Table 1).

Following the three surfactants' functionalization of the γ-$Fe_2O_3$, a notable increase in yield is seen. The improved surface-to-volume ratio of the functionalized nanoparticles can be used to explain this improvement. After just 15 minutes of interaction, the three curves exhibit an increasing tendency and reach their maximum (figure 6). This observation suggests that Cr(VI) and the adsorbent γ-$Fe_2O_3$@CnTAB have a significant interaction. γ-$Fe_2O_3$@CnTAB has the highest extraction %, which can be due to its strong hydrophobic effect, which promotes attraction. This force is present between the ammonium group's $N^+$ and $HCrO_4^-$, which is generated in an acidic media (pH = 2). The length of the hydrophobic chain in the cationic surfactantbonded to the γ-$Fe_2O_3$ nanoparticle causes this force to rise. The degree of chromium(VI) removal between hybrid nanoparticles is clarified by this explanation.

### 3.4. pH effect

The pH of the sample affects the adsorption process by causing protonation and deprotonation of the functional groups on the adsorbent surface. The impact of varying pH values (2, 7, and 9) on Cr(VI) adsorption was examinedover a 14-minute contact period, using nanoparticle concentrations of 12, 8, and 4mg/mL. Table 2 shows that, after 15 minutes of contact time, the highest Cr(VI) adsorption reached at pH 2 for the adsorbents.Table 3 shows that at acidic pH 2, the γ-$Fe_2O_3$@CnTAB composite demonstrates a greater adsorption efficiency than γ-$Fe_2O_3$. A maximum Cr(VI) removal of 96% was achieved after 15 minutes of contact, with the highest removal occurring at pH 2.

In an acidic media at pH 2, the γ-$Fe_2O_3$@CnTAB compound exhibits greater adsorption efficiency. In a basic medium at pH 9 and a neutral medium at pH 7, the amount of Cr(VI) removed was 84% and 78%, respectively, for the same quantity of adsorbent γ-$Fe_2O_3$@CnTAB (4 mg/ml). On the other hand, the removal is greaterup to 96%at pH 2.

It is clear that an acidic environment enhances Cr(VI) elimination. This is explained by the fact that the protonated amine group ($N^+$) of CTAB (γ-$Fe_2O_3$@CTABzeta potentials are positive at pH <6.4) causes the nanocomposite to become positively charged in an acidic solution. The positively charged nanocomposite efficiently retains the oppositely charged $HCrO_4^-$ ions via attraction by electrostatic force. In a basic pH, an excess of $OH^-$ competes with the Cr(VI) for binding at the anion exchange sites of the γ-$Fe_2O_3$@CTAB composite, resulting in a repulsive interaction between the Cr(VI) ions and the adsorbent surface. Additionally, the magnetic field generated by the γ-$Fe_2O_3$@CnTAB magnetic nanoparticles, along with the presence of free radicals, may contribute to the adsorption process.

Studies have demonstrated that the pH of the solution has a significant impact on the adsorption of Cr(VI).This is because the adsorbent's surface contains functional groups that vary in type and ionic state [27].

### 3.5. Salt effect

The presence of interfering ions, such as potassium nitrate ($KNO_3$) at a concentration of 0.01 g/L,had minimal effect on the adsorption of Cr(VI) ions, highlighting the strong selectivity of γ-$Fe_2O_3$@CTAB for Cr(VI). After 15 minutes, Cr(VI) removal was smaller than 70% with $KNO_3$ present, compared to 96% without it. The adsorption efficiency of Cr(VI) was reduced by 33% due to the presence of salts.

**Table 1.** Maximum % of Cr(VI) eliminated as a function of functionalizing surfactant.

| Adsorbents | $\gamma$-$Fe_2O_3$ | $\gamma$-$Fe_2O_3$@CTAB |
|---|---|---|
| percentage of chromium removed | 73% | 95% |

**Table 2.** Adsorption of Cr by $\gamma$-$Fe_2O_3$ and $\gamma Fe_2O_3$@CTAB

| | $\gamma$-$Fe_2O_3$@CTAB | $\gamma$-$Fe_2O_3$@TTAB | $\gamma$-$Fe_2O_3$@DeTAB |
|---|---|---|---|
| Cr(VI) removed. | 95% | 88% | 93% |

**Table 3.** Adsorption of Cr(VI) at different pH values

| | pH=2 | pH=7 | pH=9 |
|---|---|---|---|
| % of Cr(VI) removed | 96% | 78% | 84% |

### 3.6. Effect of Adsorbent Dosage on Cr(VI) Removal

The two adsorbents were tested at different dosages (12, 8, and 4 mg/mL) to remove Cr(VI) ions (1 mg/L) at room temperature (25.0°C ± 1.0°C) over various contact times. As the dosage of both adsorbents increased, the removal efficiency of Cr(VI) decreased. At a dosage of 12 mg/mL, $\gamma$-$Fe_2O_3$ removed 84% of Cr(VI) after 15 minutes of exposure. In contrast, the $\gamma$-$Fe_2O_3$@CnTAB composite at 4 mg/mL achieved the highest removal, capturing 94% of Cr(VI). MNPs@CnTAB nanoparticles, at an intermediate dosage of 8 mg/mL, removed 87% of Cr(VI).

## 4. Conclusion

Using a one-step coprecipitation approach, maghemite nanoparticles, namely $\gamma$-$Fe_2O_3$, were successfully produced and modified with different cationic surfactants. The ability of these hybrid nanoparticles to remove the toxic heavy metal Cr(VI) from water was evaluated. According to the study, maghemite is a useful material for adsorbing Cr(VI), albeit how well it works relies on the properties of the material and the surrounding environment. The optimization results show numerous important conclusions:

- Higher extraction efficiency is achieved by surfactants with longer alkyl chains.
- Although basic and neutral conditions are best for extraction, acidic settings nevertheless provide notable outcomes.

The ideal adsorbent dosage for Cr(VI) concentrations between 0 and 1 mg/L is 4 mg.

- The technique works well even with salts present.
- The maximal extraction may be obtained in a few minutes of contact time, demonstrating the speed of extraction.

The approach can detect Cr(VI) at concentrations as low as a few parts per million. It removes over 95% of Cr(VI) from various media. Its extraction and analysis procedure does not require the use of hazardous organic solvents and can be performed with normal laboratory equipment.

These findings highlight the potential of functionalized maghemite nanoparticles with cationic surfactants as an effective and environmentally friendly method for removing Cr(VI) from water. This approach is a viable choice for upcoming water treatment applications because of its ease of use, rapidity, and compatibility with standard laboratory apparatus. The adsorbent's long-term stability and scalability for usage in real-world applications can be investigated in more detail in future research.

**Disclosure statement:** Conflict of Interest: The authors declare that there are no conflicts of interest.

Compliance with Ethical Standards: This article does not contain any studies involving human or animal subjects.

## References


1. J J Coetzee, N Bansal, E M Chirwa, *Exposure and Health* **12** (2020).
2. M Bilal, I Ihsanullah, M Younas, M U H Shah, *Separation and Purification Technology* **278** (2021).
3. N Karimi, S A Mirbagheri, R Nouri, A Bazargan, *Results in Engineering* **17** (2023).
4. F S A Khan, N M Mubarak, M Khalid, R Walvekar, E C Abdullah, S A Mazari, S Nizamuddin, R R Karri, *Environmental Science and Pollution Research* **27** (2020).
5. H M Ali, F A Roghabadi, V Ahmadi, *Solar Energy* **255** (2023).
6. S M Rajput, M Kuddushi, A Shah, D Ray, V K Aswal, S K Kailasa, N I Malek, *Surfaces and Interfaces* **20** (2020).
7. P Kolimi, S Narala, A A A Youssef, D Nyavanandi, N Dudhipala, *Nanotheranostics* **7** (2023).
8. M Naous, A Halfadji, A Chougui, B Bounaceur, *Chemical Methodologies* (2022).
9. M Naous, J Aguiar, C C Ruiz, *Colloid and Polymer Science* **290** (2012).
10. S M Siddeeg, M A Tahoon, N S Alsaiari, M Shabbir, F B Rebah, *Current Analytical Chemistry* **17** (2021).
11. A Jawed, V Saxena, L M Pandey, *Journal of Water Process Engineering* **33** (2020).
12. Q Shen, X Xu, X Liang, C Tang, X Bai, S Shao, Q Liang, S Dong, *Environmental Research* **264** (2025).
13. Z -R Yu, M Mao, S -N Li, Q -Q Xia, C -F Cao, L Zhao, G -D Zhang, Z -J Zheng, J -F Gao, L -C Tang, *Chemical Engineering Journal* **405** (2021).
14. S Rajendran, S G Wanale, A Gacem, V K Yadav, I A Ahmed, J S Algethami, S D Kakodiya, T Modi, A M Alsuhaibani, K K Yadav, *Crystals* **13** (2023).
15. D Ramimoghadam, S Bagheri, S B Abd Hamid, *Colloids and Surfaces B: Biointerfaces* **133** (2015).
16. E N Ngouangna, M Z Jaafar, M M Norddin, A Agi, J O Oseh, S Mamah, *Journal of Molecular Liquids* **360** (2022).
17. T Rasheed, S Shafi, M Bilal, T Hussain, F Sher, K Rizwan, *Journal of Molecular Liquids* **318** (2020).
18. S Prasad, K K Yadav, S Kumar, N Gupta, M M Cabral-Pinto, S Rezania, N Radwan, J Alam, *Journal of Environmental Management* **285** (2021).
19. M Naous, F Bouanani, S Bravo, *Materials Today: Proceedings* **13** (2019).
20. D Predoi, S L Iconaru, MV Predoi, M Motelica-Heino, *Polymers* **12** (2020).

21. R Ouafi, Z Rais, M Taleb, *Desalination and Water Treatment* **180** (2020).
22. C Raji, T Anirudhan, *Water Research* **32** (1998).
23. N B Orm, *Doctoral dissertation, Université Claude Bernard-Lyon I* (2012).
24. T Tuutijärvi, J Lu, M Sillanpää, G Chen, *Journal of Hazardous Materials* **166** (2009).
25. J A Celis, O Olea Mejía, A Cabral-Prieto, I García-Sosa, R Derat-Escudero, E Baggio Saitovitch, M Alzamora Camarena, *Hyperfine Interactions* **238** (2017).
26. P Kushwaha, PChauhan, *Phase Transitions* **94** (2021).
27. P Bandara, J Peña-Bahamonde, D Rodrigues, *Scientific Reports* **10** (2020).